

N73-31609

R-743  
STRAPDOWN SYSTEM PERFORMANCE  
OPTIMIZATION TEST EVALUATIONS (SPOT)  
Final Report on Contract NAS 9-6823  
Modification 11  
by  
Richard J. Blaha and Jerold P. Gilmore  
February 1973

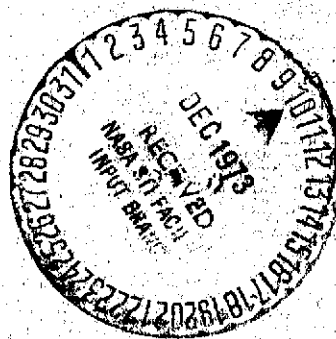
Volume 11

(NASA-CR-136083) STRAPDOWN SYSTEM  
PERFORMANCE OPTIMIZATION TEST EVALUATIONS  
(SPOT), VOLUME 2 Final Report  
(Massachusetts Inst. of Tech.) 22 p HC  
22 25

N74-12355

Unclas  
15756  
CSCL 17G G3/21

Reproduced by  
NATIONAL TECHNICAL  
INFORMATION SERVICE  
US Department of Commerce  
Springfield, VA. 22151



**CHARLES STARK DRAPER  
LABORATORY**

MASSACHUSETTS INSTITUTE OF TECHNOLOGY

CAMBRIDGE, MASSACHUSETTS, 02139

PRICES SUBJECT TO CHANGE

21

R-743

Strapdown System Performance Optimization Test Evaluations (SPOT)  
Final Report on Contract NAS 9-6823 Modification 11

by

Richard J. Blaha and Jerold P. Gilmore

VOLUME II

Charles Stark Draper Laboratory  
Massachusetts Institute of Technology  
Cambridge, Massachusetts  
02139

Approved: Jerold P. Gilmore Date: 27 Feb 1973  
J. P. GILMORE, DEPUTY ASSOCIATE DIRECTOR

Approved: Ralph B. Hoag / for Date: 27 Feb 73  
N. E. SEARS, ASSOCIATE DIRECTOR

Approved: Ralph B. Hoag / for Date: 27 Feb 73  
D. G. HOAG, DEPUTY DIRECTOR

### Acknowledgement

This report was prepared under DSR Project 55-29435 sponsored by the Manned Spacecraft Center of the National Aeronautics and Space Administration under contract NAS 9-6823.

The publication of this report does not constitute approval by the National Aeronautics and Space Administration of the findings or the conclusions contained herein. It is published only for the exchange and stimulation of ideas.

### Abstract

A three axis inertial system is packaged in an Apollo gimbal fixture for fine grain evaluation of strapdown system performance in dynamic environments. These evaluations have provided information to assess the effectiveness of real-time compensation techniques and to study system performance tradeoffs to factors such as quantization and iteration rate. The strapdown performance and tradeoff studies conducted in this program include:

1. Compensation models and techniques for the inertial instrument first-order error terms were developed and compensation effectivity was demonstrated in four basic environments; single and multi-axis slew, and single and multi-axis oscillatory.
2. The theoretical coning bandwidth for the first-order quaternion algorithm expansion was verified. The pseudo coning bandwidth was measured and identified to be a combined function of the attitude algorithm's coning bandwidth and the OA coupling compensation algorithm's bandwidth.
3. Gyro loop quantization was identified to affect proportionally the system attitude uncertainty.
4. Land navigation evaluations identified the requirement for accurate initialization alignment in order to pursue fine grain navigation evaluations.

## VOLUME I

### Table of Contents

#### Section

1.0	Introduction.....	1-1
2.0	Test Facility.....	2-1
2.1	Introduction.....	2-1
2.2	Strapdown Instrument Test Package.....	2-4
2.3	Pulse Torque Electronics.....	2-8
2.3.1	Pulse Burst Compensation.....	2-16
2.4	Resolver to Digital Encoder.....	2-16
2.5	Computational Facility .....	2-19
2.5.1	Introduction.....	2-19
2.5.2	Serial Data Link.....	2-23
2.5.3	Pulse Torque Electronics.....	2-23
2.5.4	Interpolator.....	2-24
2.5.5	Resolver to Digital Encoder.....	2-24
2.5.6	Test Sequencer.....	2-24
2.6	Support Electronics.....	2-25
3.0	Inertial Instrument and Error Parameters .....	3-1
3.1	16 Permanent Magnet Pulsed Integrating Pendulous Accelerometer (16 PM PIP).....	3-1
3.1.1	Physical Description.....	3-1
3.1.2	Principle of Operation.....	3-1
3.1.3	Accelerometer Model .....	3-5
3.2	18 Integrating Inertial Gyro Mod B (18 IRIG).....	3-5
3.2.1	Physical Description.....	3-5
3.2.2	Principle of Operation.....	3-8
3.2.3	Gyroscope Model .....	3-11
3.2.3.a	Anisoinertia.....	3-13
3.2.3.b	Scale Factor Linearity.....	3-15

## Table of Contents (Cont)

	3.2.3.c	SRA Cross Coupling Error.....	3-15
	3.2.3.d	OA Coupling.....	3-25
	3.2.4	Attitude Storage.....	3-28
	3.2.5	Fine Attitude Quantization With Hybrid Operations ..	3-30
4.0		Software Development .....	4-1
4.1		Introduction.....	4-1
4.2		Calibration Software.....	4-1
	4.2.1	Data Acquisition.....	4-1
	4.2.2	Data Transfer .....	4-4
4.3		Compensation, Attitude, and Velocity Algorithms.....	4-5
	4.3.1	Introduction .....	4-5
	4.3.2	Compensation Algorithms .....	4-5
		4.3.2.a Gyro Compensation Algorithm .....	4-7
		4.3.2.b Accelerometer Compensation Algorithm.....	4-11
	4.3.3	Attitude Algorithm .....	4-12
	4.3.4	Velocity Algorithm .....	4-14
	4.3.5	Algorithm Evaluation.....	4-14
		4.3.5.a Small Angle Error Studies.....	4-15
		4.3.5.b Pseudo Coning Drift.....	4-19
		4.3.5.c Coning .....	4-20
		4.3.5.d Algorithm Slewing Error .....	4-23
		4.3.5.e Algorithm Round-off Error .....	4-25
4.4		Error Quaternion .....	4-25
4.5		Land Navigation.....	4-27
4.6		Diagnostic and IBM 360/75 Programming.....	4-29
5.0		Test Results .....	5-1
5.1		Calibration Results.....	5-1
	5.1.1	Introduction .....	5-1
	5.1.2	Gimbal Calibration .....	5-1
	5.1.3	Static Calibration .....	5-4
	5.1.4	Dynamic Calibration.....	5-8
		5.1.4.a Gyro Scale Factor and Alignment.....	5-8
		5.1.4.b Anisoinertia .....	5-9
		5.1.4.c Centripetal Accelerometer .....	5-10

## Table of Contents (Cont)

5.2	Compensation Results.....	5-13
5.2.1	Introduction.....	5-13
5.2.2	Bandwidth Studies .....	5-15
5.2.2.a	Coning.....	5-15
5.2.2.b	Pseudo Coning.....	5-23
5.2.3	Anisoinertia and SRA Cross Coupling .....	5-33
5.2.4	Algorithm Dynamic Uncertainty.....	5-39
5.2.4.a	Attitude Uncertainty.....	5-39
5.2.4.b	Bandwidth Effects.....	5-43
5.2.5	Pulse Burst Compensation.....	5-45
5.2.6	Scale Factor Linearity.....	5-47
5.3	Land Navigation Results.....	5-50
5.3.1	Latitude and Longitude Errors.....	5-50
5.3.2	Oscillatory Test Results .....	5-55
5.3.3	Slew Test Results .....	5-56
5.3.4	Summary.....	5-61
5.4	Multi-Position Accelerometer Evaluations .....	5-62
5.4.1	Introduction .....	5-62
5.4.2	Fourier Series Analysis.....	5-62
5.4.3	Least Square Analysis .....	5-64
5.4.4	Accelerometer Model Evaluation.....	5-65
5.4.5	Sixteen Position to Four Position Data Comparison	5-69
5.5	Program Milestones.....	5-72
6.0	Conclusions and Recommendations.....	6-1

## APPENDICES A - W

VOLUME II

TABLE OF CONTENTS

1.0	Introduction.....	1-1
2.0	Calibration Data.....	1-1

PRECEDING PAGE BLANK NOT FILMED



## LIST OF ILLUSTRATIONS (VOLUME II)

Figure		Page
2.1	X Axis Accelerometer Alignment.....	1-4
2.2	Y Axis Accelerometer Alignment.....	1-5
2.3	Z Axis Accelerometer Alignment.....	1-6
2.4	Accelerometer Bias.....	1-8

PRECEDING PAGE BLANK NOT FILMED

## 1.0 Introduction

This volume presents the accelerometer performance data that was obtained as part of the dynamic evaluations conducted with the SPOT (Strapdown Performance Optimization Test) system. This program is funded under NASA contract NAS 9-6823, modification 11 (see Appendix A for the program's objectives and mechanization description).

The accelerometer tested is the Charles Stark Draper Laboratory designed size 16 permanent magnet pulsed integrating pendulous accelerometer (16PMPIP). The accelerometer is mechanized with a ternary pulse torque-to-balance loop with a quantization of 1 cm/sec per pulse. At a repetition rate of 4800 pps the accelerometer dynamic range is 5g.

The pulse torque electronics are separated from the accelerometer by the gimbal slip rings and connectors. One of the program's initial design concerns was the effect of this implementation on system performance. The data presented in this report has been statistically evaluated and compared to similar data obtained with the Strapdown Redundant Inertial Unit (SIRU) where proximity packaging concepts are utilized. Except for accelerometer alignment, the data from both systems agree with each other. Hence, the gimbal system mechanization has proven to have little effect on scale factor and bias variability. The variability difference observed in the accelerometer alignment calibration data is traceable to the gimbal alignment uncertainties. In fact, a linear correlation is observed between the gimbal alignment data and the accelerometer alignment data. This correlation is useful for monitoring the gimbal calibration status using the accelerometer outputs.

## 2.0 Calibration Data

The accelerometer calibration is achieved using a four position procedure (See Appendix B). The calibration model (Equation 2.1) includes an accelerometer null bias, ( $B_0$ ) two alignment angles ( $A_{ORA}$  and  $A_{PA}$ ) and separate scale factors for positive (SF+) and negative (SF-) accelerometer inputs.

$$\underbrace{\frac{A_o}{SF^+ \text{ or } SF^-}}_{\text{indicated output}} = \underbrace{A_i}_{\text{input axis acceleration}} + \underbrace{B_o}_{\text{accelerometer bias}} + \underbrace{A_{ORA} a_P - A_{PA} a_O}_{\text{alignment error}}$$

Second order terms, such as cross axis coupling scale factor non-linearity, were evaluated using least square modeling techniques (see Section 5.4 of Volume I) and determined to be insignificant.

Through the utilization of a H316 minicomputer, an automatic calibration facility was implemented. Overnight accelerometer calibrations were conducted periodically and a voluminous accumulation of data was accomplished with the disk storage for later statistical and trend analysis.

During the seventeen month period, March 71 to July 72, approximately 300 calibrations were achieved. From this data, the null bias one sigma ( $1\sigma$ ) value for a three day period was computed and determined to be in the range 0.001 - 0.003 cm/sec<sup>2</sup>. This stability is within the limits required for the maintenance of a calibration baseline to assure the quality of strapdown performance.

Longer term statistics were compiled for an approximate one month period during which no system shutdowns or cooldowns were experienced. Hence, the data represents accelerometer performance in benign test periods. This data is presented to establish accelerometer loop performance with the ternary pulse torque electronics physically separated by the gimbal slip rings from the instrument.

The one sigma ( $1\sigma$ ) data is summarized in Table 2.1 with a comparison to similar data obtained with a redundant strapdown system (SIRU), a system mechanization where the accelerometers and electronics are together.

TABLE 2.1 STATISTICAL DATA COMPARISON

	SPOT 1 $\sigma$ for one month period no(cooldown)	SIRU 1 $\sigma$ for 1-6 months no cooldown, or mounting change
Scale Factor	13-20 ppm	15 ppm
Null Bias	0.003 - 0.006 cm/sec <sup>2</sup>	0.006 cm/sec <sup>2</sup>
Alignment	0.020 mrad	0.010 mrad

Observe that the scale factor and null bias stabilities are identical for both systems, however, the gimbal system's alignment uncertainty is twice the SIRU system's. Hence, separation of the pulse torque electronics from the accelerometers has little impact on accelerometer performance which implies that the signal magnitudes were sufficiently above the gimbal noise levels.

The difference in alignment is attributed to the uncertainties of the gimbal alignment. The correlation between the accelerometer and the gimbal alignment is also seen in the accelerometer calibration data. Figure 2.1, 2.2, and 2.3 are the time profiles for the accelerometer Input Axis alignment calibration for the period March 71 to August 72. Observe the step change in the accelerometer's alignment on 9 August 1971 and 26 September 1971.

The average alignment shift observed in all of the accelerometer data is 0.10 milliradian which is fifty times the one month sigma alignment with no cooldowns experienced. The reason for the alignment shift is attributed to a gimbal alignment change that occurs during the system cooldown. On 9 August 1972 the system temperature was reduced to room temperature in order to start gyro MB2. During the cooldown, the inner and middle gimbal resolver alignments shifted 0.18 milliradians and the inner gimbal orthogonality alignment shifted 0.01 milliradian. These gimbal alignment shifts are reflected in the accelerometer alignment data, which also corresponds in magnitude to the accelerometer alignment shift. On 26 September 1972, the gimbal alignment was re-certified and the accelerometer alignment was restored its baseline value which was established prior to the 9 August cooldown.

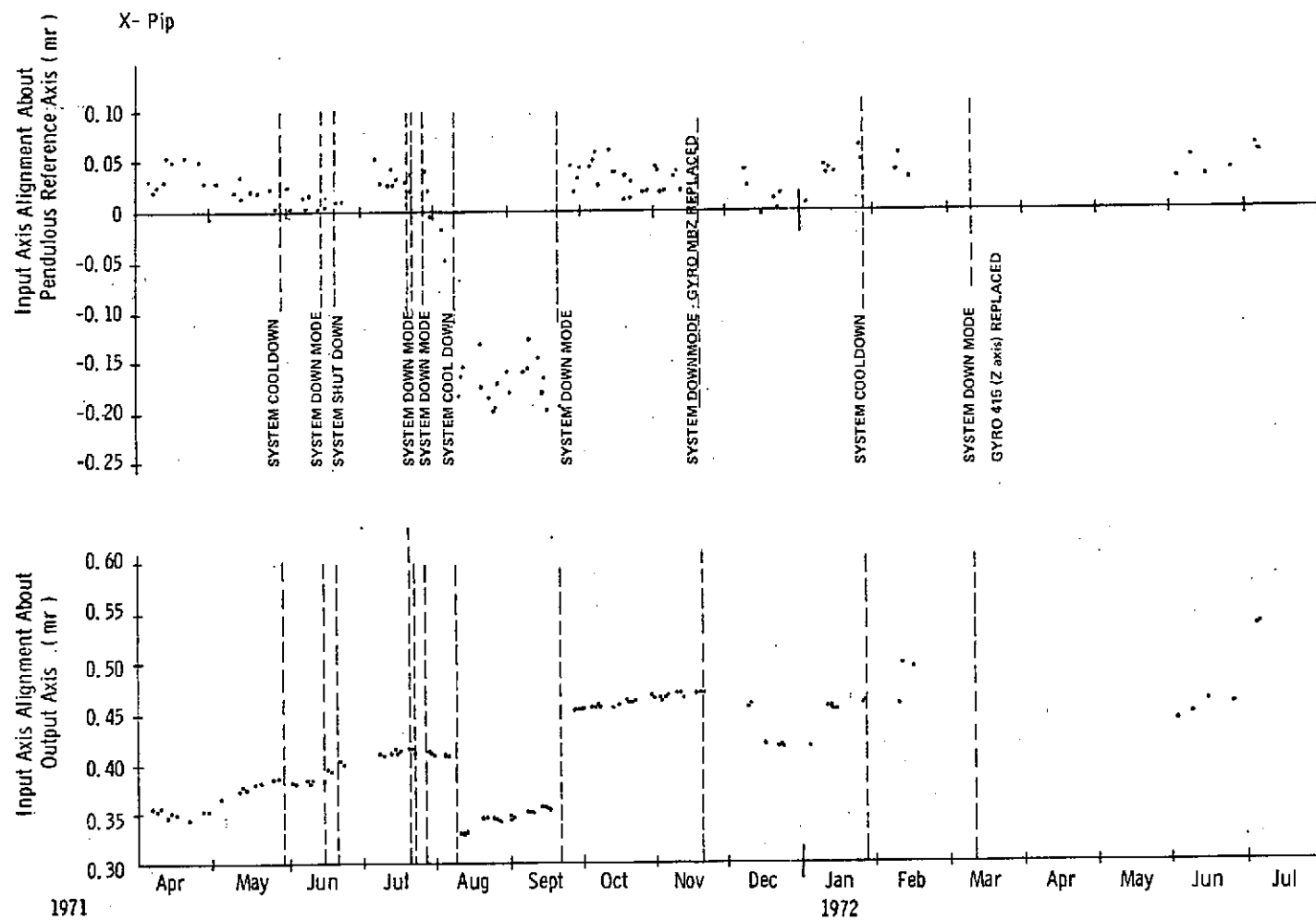


Fig. 2.1 X-Axis Accelerometer Alignment.

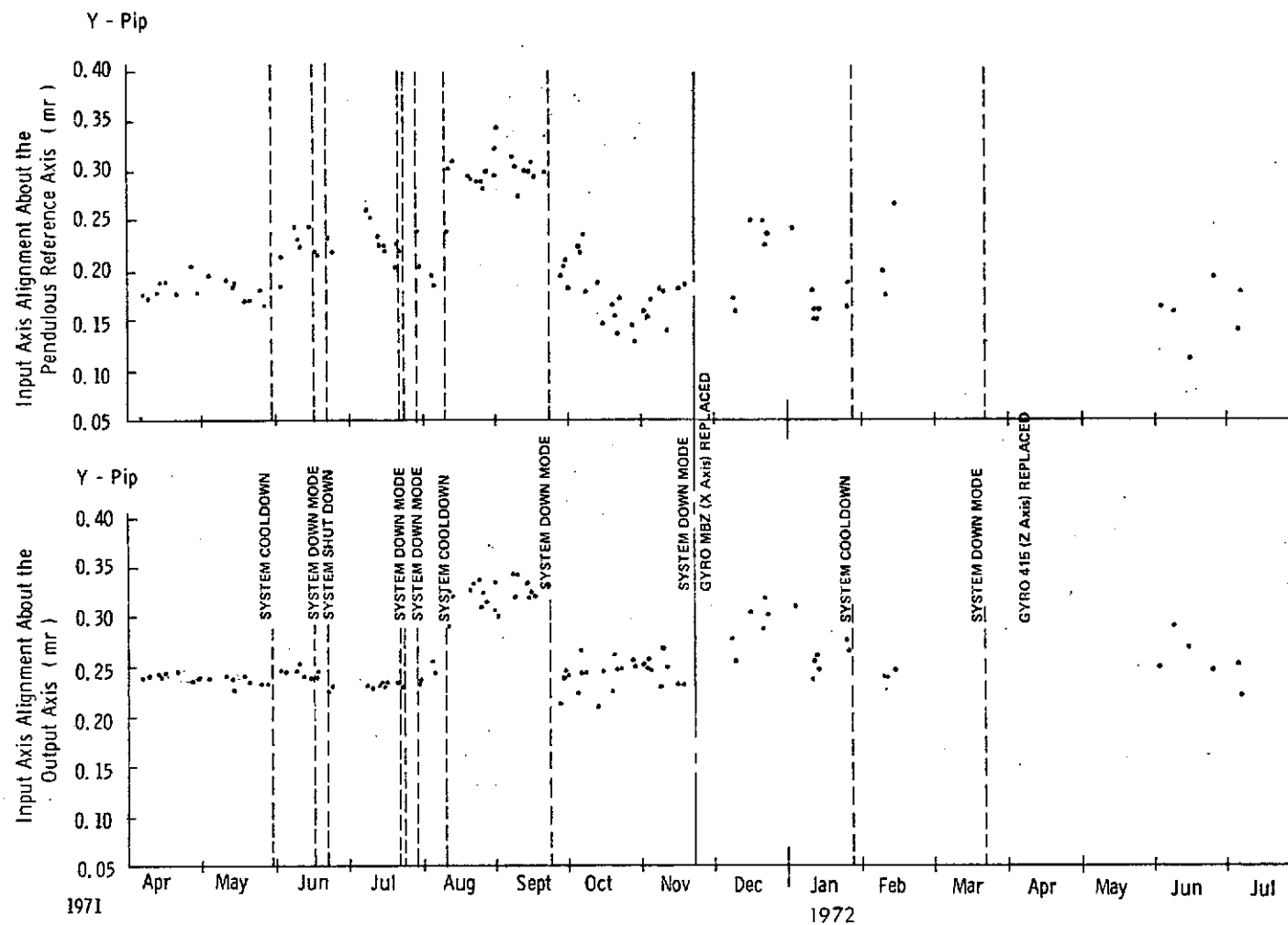


Fig. 2.2 Y-Axis Accelerometer Alignment

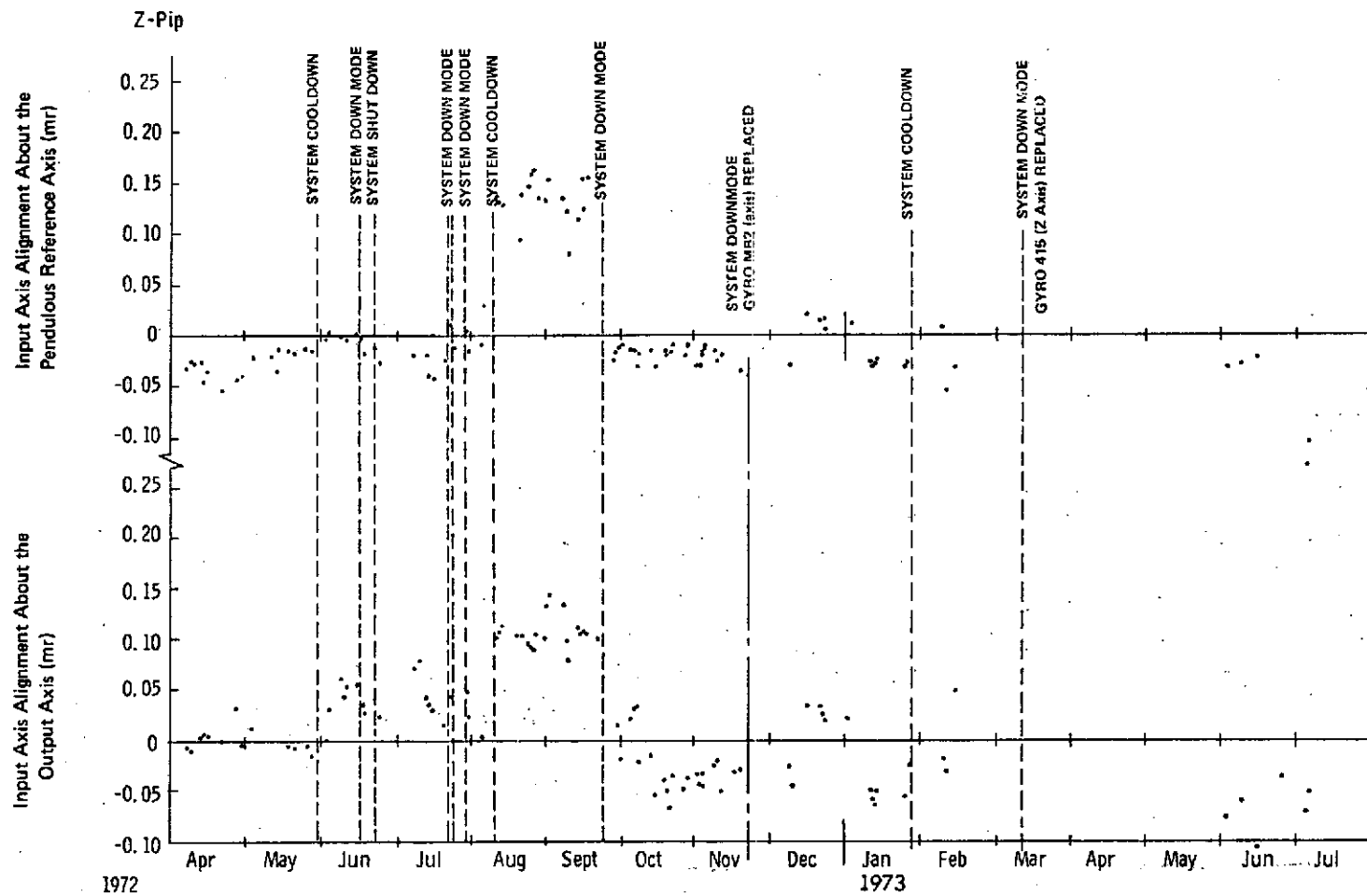


Fig. 2.3 Z-Axis Accelerometer Alignment.

This interdependency between the accelerometer alignment and the gimbal alignment has useful applications. Rather than calibrating the gimbal system on a periodic basis, a task that requires considerable time, calibration is only necessary when the accelerometer data indicates that it is warranted. Of additional interest is the possibility that the accelerometer alignment data can be used in an adaptive process to correct gimbal alignment anomalies. Thus, a system alignment capability based on accelerometer inputs may exist and therefore warranting future study of possible implementation.

In Figure 2.1 observe the exponential drift of the Input Axis alignment about the Output Axis ( $SO_X$ ). This slowly drifting alignment is attributed to a stress release in the accelerometer's alignment fixture about the Output Axis. A stress release in the gimbal structure is discounted because the same exponential change is not observed in any of the other accelerometer data.

Figure 2.4 gives the profile of the null bias calibration (in  $\text{cm/sec}^2$ ) for all three accelerometers. In general, accelerometer null bias is observed to be invariant to discontinuities in the system operation such as downmoding from voltage transients and overnight system cooldowns. On 10 August 72, during an overnight cooldown both the X and Y axis accelerometers experienced a 0.02  $\text{cm/second}$  permanent shift in the null bias. This shift is attributed to changes in the flex lead or magnetic torques of the suspension or signal generator fields.



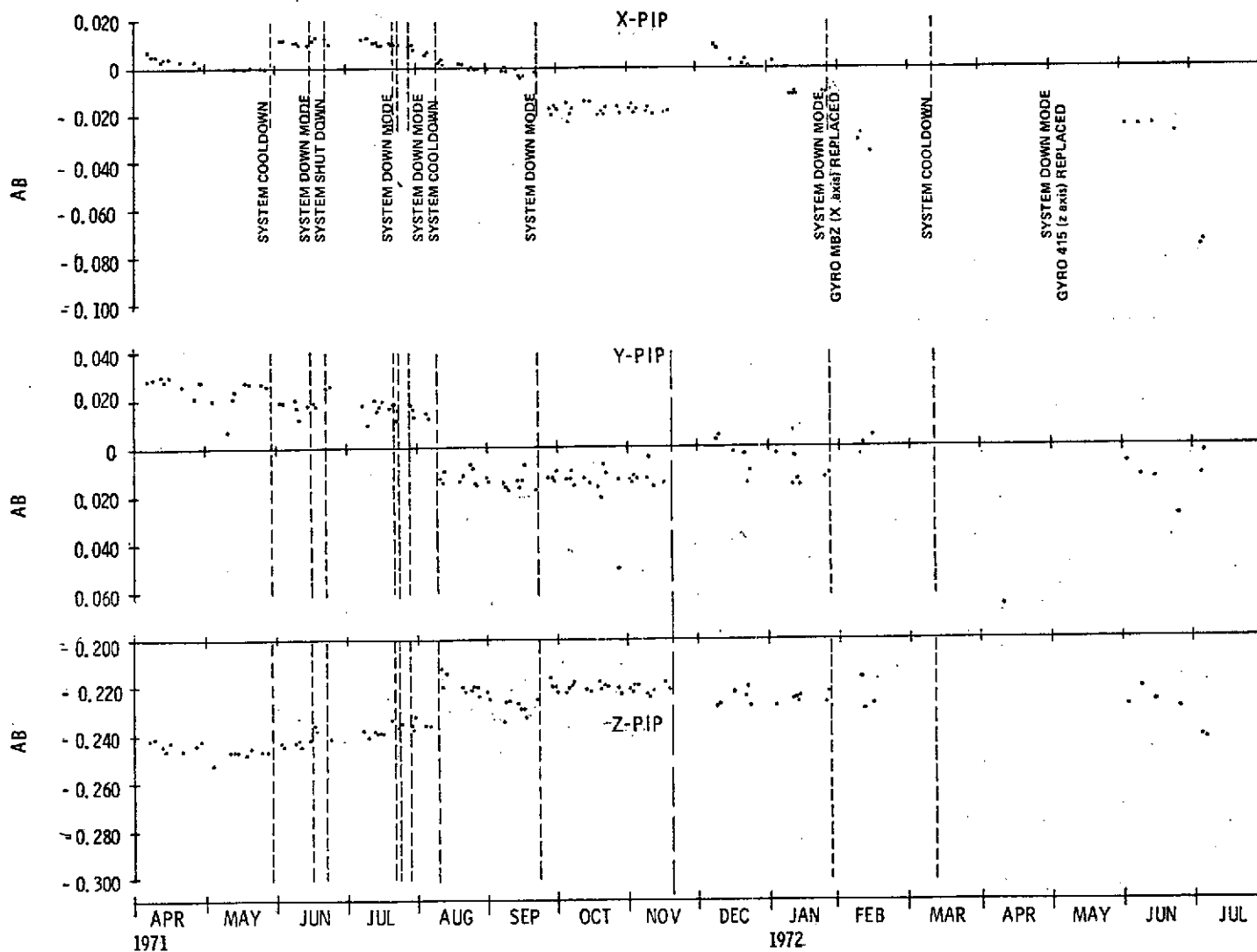


FIGURE 2.4 - ACCELEROMETER BIAS CALIBRATION

## Appendix A

### Description

The SPOT system is a three axis strapdown system, packaged in an Apollo gimbal system to evaluate strapdown performance in dynamic environments. The strapdown system that was implemented comprises three size 18 Integrating Inertial Gyro Modification B gyros (18 IRIG Mod B), and three size 16 permanent-magnet-pulsed-integrating pendulous accelerometers (16 PM PIP). All inertial instruments operate in a ternary pulse-to-balance torque mode. The gyro torque loops are implemented with compensation to suppress multiple pulse transients. Interpolators, which are basically analog-to-digital converters, monitor the gyro SG output to quantize either the gyro float hangoff or attitude information. The interpolator's mode of operation is computer controlled. Figure A-1 shows the principle components of the SPOT system.

An H316 mini-computer is used extensively in the SPOT system for automatic instrument calibration and for real time processing of the inertial instrument compensation algorithms and attitude maintenance system.

### Objective

The objective of the SPOT program is to effect a fine grain test evaluation of a strapdown system in a dynamic environment to the effectivity of instrument error compensation techniques and system performance response to different algorithm iteration rates and quantization effects. To achieve this program objective a test facility was developed that enabled the introduction of a broad spectrum of multiple axis slew and oscillatory inputs to an experimental three axis gyro and accelerometer strapdown test package. The package was operated in real time with a general purpose mini-computer that included extensive compensation and strapdown algorithm software. Using this capability and corresponding software models a wide band performance evaluation of the torque-to-balance strapdown mechanization was effected. The resultant test and trade-off performance findings presented in the body of this report provides a fuller appreciation of the strapdown error propagation characteristics and identifies the opportunities for further strapdown refinement and advanced software development.

# SPOT SYSTEM CONFIGURATION

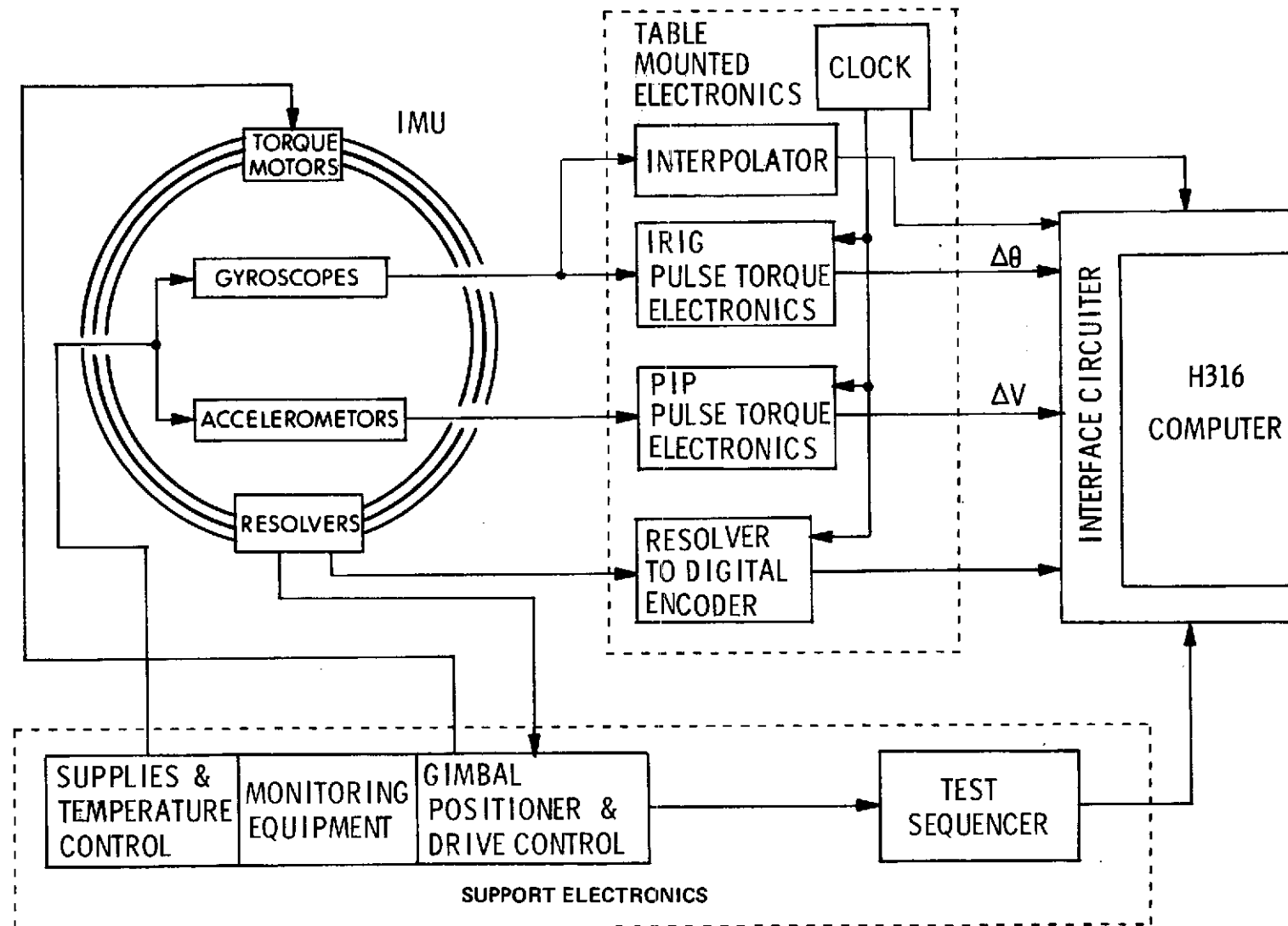


Fig. A-1 SPOT System Configuration

## Appendix B

### Accelerometer Calibration

#### A. Definitions

$K_{ij}$  - average accelerometer pulse rate for the  $i^{\text{th}}$ , accelerometer ( $i = x, y, \text{ or } z$ ) in the  $j^{\text{th}}$  calibration position ( $j = 1, 2, \dots 6$ ). Each  $k_{ij}$  is calculated by averaging the accumulated accelerometer pulses over the calibration interval.

$g$  - gravitational acceleration

$\epsilon_{ik}$  - gimbal and test table alignment errors.

#### B. Accelerometer Calibration Equations

The accelerometer parameters are solved as a function of the measured pulse rates. Trigonometric identities and small angle approximations have been used. The average scale factor and the scale factor difference are defined as:

$$SFA_i = \frac{SF_i^+ + SF_i^-}{2}$$

$$\Delta SF_i = SF_i^+ - SF_i^-$$

The isolated PIPA parameters are shown to be:

a) Average Scale Factor,  $SFA_i$  (cm/sec/pulse)

$$SFAX = \frac{2g}{KX1-KX2}$$

$$SFAY = \frac{2g}{KY3-KY4}$$

$$SFAZ = \frac{2g}{KZ6-KZ5}$$

b) Bias,  $AB_i$  (cm/sec<sup>2</sup>)

$$ABX = 1/2 SFAX (KX5+KX6) + g (\epsilon_{MGA})$$

$$= 1/2 \text{ SFAX } (KX3+KX4) + g (\epsilon_{TT} + \epsilon_{fx} + \epsilon_{OGR})$$

$$\text{ABY} = 1/2 \text{ SFAY} (KY1+KY2)$$

$$= 1/2 \text{ SFAY } (KY5+KY6) + g (\epsilon_{TT} + \epsilon_{fx} + \epsilon_{OGR})$$

$$\text{ABZ} = 1/2 \text{ SFAZ } (KZ3+KZ4)$$

$$= 1/2 \text{ SFAZ } (KZ1+KZ2) - g (\epsilon_{TT} + \epsilon_{fx} + \epsilon_{OGR})$$

- c) Scale Factor Difference between  $\pm 1$  g positions,  $\Delta \text{SF}_i$   
(cm/sec/pulse)

$$\Delta \text{SFX} = \frac{4\text{ABX} - 2\text{SFAX } (KX1+KX2)}{(KX1-KX2)}$$

$$\Delta \text{SFY} = \frac{4\text{ABY} - 2\text{SFAY } (KY3+KY4)}{(KY3-KY4)}$$

$$\Delta \text{SFZ} = \frac{4\text{ABZ} - 2\text{SFAZ } (KZ6+KZ5)}{(KZ6-KZ5)}$$

- d) Input axis misalignment due to a rotation about the output axis  $\text{SO}_i$  (radians)

$$\text{SOX} = \frac{\text{SFAX } (KX3-KX4)}{2g} + \epsilon_{IGA}$$

$$\text{SOY} = + \frac{\text{SFAY } (KX5-KX6)}{2g} - \epsilon_{IGA}$$

$$\text{SOZ} = - \frac{\text{SFAZ } (KZ3-KZ4)}{2g} + \epsilon_{TR} - \epsilon_{fz}$$

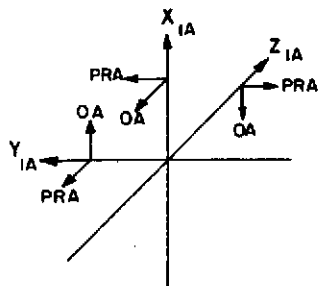
- e) Input axis misalignment due to a rotation about the negative pendulum axis,  $\text{SP}_i$  (radians)

$$\text{SPX} = \frac{\text{SFAX } (KX5-KX6)}{2g} + \epsilon_{TR} - \epsilon_{fz} + \epsilon_{IGR}$$

$$\text{SPY} = \frac{\text{SFAY } (KY1-KY2)}{2g} + \epsilon_{TR} - \epsilon_{fz} + \epsilon_{MGR}$$

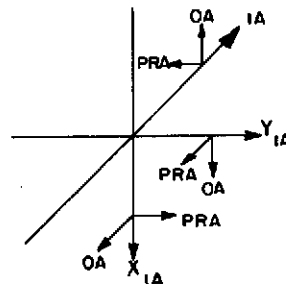
$$\text{SPZ} = - \frac{\text{SFAZ } (KZ1-KZ2)}{2g} - \epsilon_{IGR}$$

CAL #1



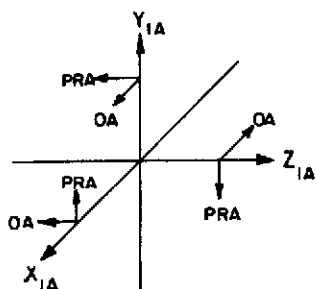
OGA = 0  
IGA = 0  
MGA = 270°

CAL #2



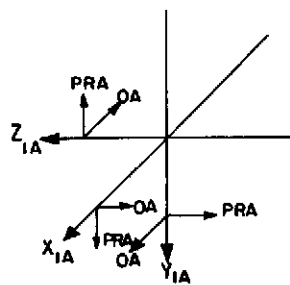
OGA = 0  
IGA = 0  
MGA = 270°

CAL #3



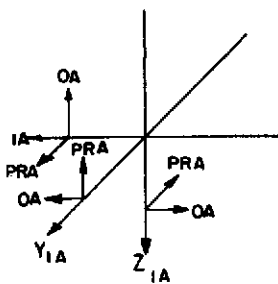
OGA = 0  
IGA = 270°  
MGA = 0

CAL #4



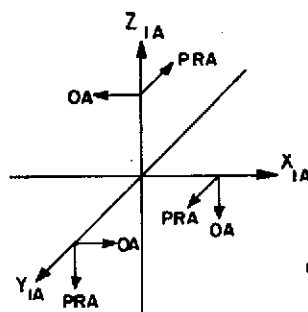
OGA = 0  
IGA = 270°  
MGA = 180°

CAL #5



OGA = 270°  
IGA = 0  
MGA = 180°

CAL #6



OGA = 90°  
IGA = 0  
MGA = 0

Fig. B-1 Cardinal Calibration Positions- Accelerometer Orientation.